nature portfolio

https://doi.org/10.1038/s41893-022-00847-2

Supplementary information

Scalable manufacturing of sustainable packaging materials with tunable thermoregulability

In the format provided by the authors and unedited

Scalable manufacturing of sustainable packaging materials with tunable thermoregulability

Badshah, M.A., et al.

Supplementary Information

Supplementary Note 1. Estimated Manufacturing Costs for Metallized Sheets and the Composite Materials.

The manufacturing costs for the composite materials were estimated according to well-known and extensive precedent established for the manufacturing of laminates, composites, coated sheets, and metallized films in the packaging (and other) industries[S1–S12].

The total cost of manufacturing for metallized polymer sheets $C_{Total,PS}$ can be estimated by using the following equation, in which tooling costs are omitted for simple geometries[S8–S12]:

$$C_{Total,PS} = C_{L,PS} + C_{MT,PS} + C_{MF,PS} \tag{1}$$

where $C_{L,PS}$ represents the labor costs associated with manufacturing, $C_{MT,PS}$ represents the total material costs for a manufacturing process, and $C_{MF,PS}$ represents general manufacturing expenses.

The labor costs $C_{L,PS}$ incorporate all activities required for personnel to produce metallized polymer sheets and can be generally estimated by using the following equation[S8–S12]:

$$C_{L,PS} = W_{hourly} + \sum_i t_{activity,i} \tag{2}$$

where W_{hourly} represents the hourly wage and $t_{activity,i}$ represents the time associated with any specific manufacturing activity i.

The material costs $C_{MT,PS}$ incorporate all direct and indirect costs associated with producing metallized polymer sheets and can be estimated by using the following equation[S8–S12]:

$$C_{MT,PS} = C_{M,metal} + C_{M,polymer} \tag{3}$$

where $C_{M,metal}$ represents the required amount of metal (both deposited and wasted) and $C_{M,polymer}$ represents the required amount of polymer (both processed and wasted).

The manufacturing expenses $C_{MF,PS}$ incorporate the general infrastructural expenses associated with producing metallized polymer sheets and can be estimated by using the following equation[S8–S12]:

$$C_{MF,PS} = C_{equipment} + \sum_i C_{other\ overhead,i} \quad (4)$$

where $C_{equipment}$ represents the equipment (capital asset) acquisition and maintenance costs and $C_{other\ overhead,i}$ represents common location-specific overhead costs associated with manufacturing requirements i (e.g., warehousing, water, electricity, taxes, and analogous others).

The costs described above for the manufacturing of metallized polymer sheets are well known to vary for different metal and polymer combinations, as well as across geographic locations due to logistical and infrastructural constraints, thus making it most appropriate to represent the relative contribution of each cost component with a general range. For example, the labor costs $C_{L,PS}$ typically constitute 3 % to 12 % of the total amount, the material costs $C_{MT,PS}$ typically constitute 60 % to 73 % of the total amount, and the manufacturing expenses $C_{MF,PS}$ typically constitute 24 % to 28 % of the total amount (**Supplementary Table 1**)[S11]. Consequently, for metallized polymer sheets, the labor costs $C_{L,PS}$ span a range of ~ \$ 0.002 to ~ \$ 0.018 per square meter, the material costs $C_{MT,PS}$ span a range of ~ \$ 0.04 to ~ \$ 0.09 per square meter (due to economies of scale), and the manufacturing expenses $C_{MF,PS}$ span a range of ~ \$ 0.013 to ~ \$ 0.042 per square meter (**Supplementary Table 1**)[S11,S12]. The total cost for the manufacturing of metallized polymer sheets $C_{Total,PS}$ is therefore estimated as ~ \$ 0.055 to ~ \$ 0.15 per square meter from equation *(1)* (**Supplementary Table 1**).

The total cost for the manufacturing of our composite materials $C_{Total,Composite}$ can be estimated by using a modified version of equation *(1)*:

$$C_{Total,Composite} = C_{L,Composite} + C_{MT,Composite} + C_{MF,Composite} \quad (5)$$

where $C_{L,Composite}$ represents the labor costs associated with manufacturing, $C_{MT,Composite}$ represents the total material costs for a manufacturing process, and $C_{MF,Composite}$ represents general manufacturing expenses.

The total cost for the manufacturing of our composite materials $C_{Total,Composite}$ can be calculated by making reasonable assumptions based on the fact that our manufacturing approach requires standard industrial equipment and routine fabrication processes, e.g., electron beam evaporation, spraycoating, and delamination (see Methods). Therefore, the labor costs, e.g., training, associated with the manufacturing of our composites are assumed to be roughly equivalent to those established for the manufacturing of metallized polymer sheets, i.e., $C_{L,Composite} \approx C_{L,PS}$, and moreover, the general expenses associated with the manufacturing of our composites are assumed to be roughly equivalent to those established for the manufacturing of metallized polymer sheets, i.e., $C_{MF,Composite} \approx C_{MF,PS}$. Consequently, $C_{Total,Composite}$ can be estimated by updating equation *(5)* to:

$$C_{Total,Composite} = C_{L,PS} + C_{MT,PS} + C_{MF,Composite} \tag{6}$$

The material costs $C_{MT,Composite}$ associated with producing our composite materials can be estimated by using a modified version of equation *(3)*:

$$C_{MT,Composite} = C_{M,metal} + C_{M,polymer} + C_{M,solvent} \tag{7}$$

where $C_{M,metal}$ represents the required amount of copper (both deposited and wasted), $C_{M,polymer}$ represents the required amount of SEBS (both processed and wasted), and $C_{M,solvent}$ represents the overall required amount of toluene.

For our composite materials, the percent contributions of labor costs $C_{L,Composite}$, material costs $C_{MT,Composite}$, and manufacturing expenses $C_{MF,Composite}$ to the total costs $C_{Total,Composite}$ are estimated as comparable to those established for metallized polymer sheets. Thus, the labor costs $C_{L,Composite}$ span a range of ~ \$ 0.002 to ~ \$ 0.018 per square meter, the material costs $C_{MT,Composite}$ obtained from vendor quotes (without accounting for economies of scale) span a range of ~ \$ 0.1 to ~ \$ 0.13 per square meter, and the reported manufacturing expenses $C_{MF,Composite}$ span a range of ~ $ 0.013 to ~ $ 0.042 per square meter (**Supplementary Table 1**). The total cost for the manufacturing of our composite materials $C_{Total,Composite}$ is therefore very conservatively estimated as ~ $ 0.115 – ~ $ 0.19 per square meter from equation *(6)* (**Supplementary Table 1**).

Supplementary Note 2. Theoretical Calculation of Heat Transfer Between Various Types of Coffee-Filled Cups and the Surrounding Environment.

The transfer of heat between a coffee-filled cup that was either uncovered (bare) or covered with different materials and the surrounding environment was computationally analyzed according to well-known procedures and standard equations. The generalized model accounted for the conductive, convective, and radiative heat transfer mechanisms anticipated in realistic situations but also made some reasonable assumptions (which are listed below) to facilitate and simplify the overall analysis. First, the cup is completely filled with coffee, and the geometry of the cup is approximately cylindrical. Second, the thermal and physical properties of coffee resemble those of water. Third, there is no mass transport from the cup to the surroundings, i.e., coffee is not lost through evaporation. Fourth, the metallized sides of the Mylar sheets and composites are in direct contact with the exterior of the cup. Fifth, the composite material can be represented as a polymer matrix coated with a planar copper film, i.e., the embedded copper nanostructures are omitted for simplicity. Sixth, the convective heat transfer coefficient and other physical parameters for coffee (effectively water), the convective heat transfer coefficient of air, the thermal conductivity of paper, the thermal conductivity of copper, the thermal conductivity of the SEBS polymer, and the thermal conductivity of the metallized Mylar sheet can be approximated by reported literature values[S13–S18]. Seventh, the thicknesses of the unstrained composite materials, SEBS polymer films, and metallized Mylar sheets are obtained from experimental measurements, and the relatively small changes in the thickness of the composite materials for applied strains of $\leq 30\ \%$ are neglected. Eighth, the average emittance values of the uncovered (bare) cup and the SEBS polymer film-covered, metallized Mylar sheet-covered, and unstrained or strained composite material-covered cups can be approximated from experimental measurements of the corresponding transmittance and reflectance values. Last, the emittance of the environment is unity (one), i.e., the environment behaves as a black body. Based on the above reasonable assumptions, the coffee-filled cups are approximated by the configuration schematically illustrated in **Supplementary Figure 13**. The estimated, measured, and calculated parameters associated with this configuration are defined in **Supplementary Table 2** and **Supplementary Table 3**. The equations and definitions used for the calculations are described further below.

The emittance ε was calculated according to Kirchhoff's Law of Thermal Radiation by using the following equation:

$$\varepsilon = \alpha = 1 - \tau - \rho \qquad (8)$$

where α is the absorptance, τ is the transmittance, and ρ is the reflectance.

The radiative heat transfer coefficient h_{rad} was calculated according to Newton's Law of Cooling and the Stefan-Boltzmann Law by using the following equation:

$$h_{rad} = \varepsilon\sigma(T_{external}^2 + T_{environment}^2)(T_{external} + T_{enviroment}) \qquad (9)$$

where $T_{external}$ is the temperature of the outer surface of the composite-covered cup, $T_{environment}$ is the temperature of the environment, σ is the Stefan-Boltzmann constant, and ε is the emittance of the outer surface of the composite-covered cup.

The average radiative heat transfer coefficient $h_{rad,avg}$ was calculated according to the following equation:

$$h_{rad,avg} = \frac{h_{rad}(T_{external}=T_{internal}(t=0)) + h_{rad}(T_{external}=T_{environment})}{2} \qquad (10)$$

where $T_{internal}(t = 0)$ is the initial coffee temperature and t is time.

The overall effective heat transfer coefficient h_{eff} for the composite-covered cup was calculated according to the following equation:

$$h_{eff} = h_{conv,e} + h_{rad,avg} \tag{11}$$

where $h_{conv,e}$ is the convective heat transfer coefficient of air.

The temperature of the coffee inside the composite-covered cup $T_{internal}(t)$ was calculated according to Fourier's Law for cylindrical objects by using following equation:

$$T_{internal}(t) = \frac{q(t)}{2\pi r_1 L h_{coffee}} + T_{c/p}(t) \tag{12}$$

where $q(t)$ is the total heat flow rate, r_1 is the inner radius of the paper cup, L is the height of the paper cup, h_{coffee} is the convective heat transfer coefficient of coffee (water), and $T_{c/p}(t)$ is the temperature of the coffee in contact with the inner wall of the paper cup.

The temperature of the coffee in contact with the inner wall of the paper cup $T_{c/p}(t)$ was calculated according to Fourier's Law for cylindrical objects by using the following equation:

$$T_{c/p}(t) = \frac{q(t)\, ln\frac{r_2}{r_1}}{2\pi L k_p} + T_p(t) \tag{13}$$

where r_2 is the outer radius of the paper cup, k_p is the thermal conductivity of paper, and $T_p(t)$ is the temperature of the outer wall of the paper cup in contact with the copper.

The temperature of the outer wall of the paper cup in contact with the copper $T_p(t)$ was calculated according to Fourier's Law for cylindrical objects by using the following equation:

$$T_p(t) = \frac{q(t)\, ln\frac{r_3}{r_2}}{2\pi L k_{Cu}} + T_{Cu}(t) \tag{14}$$

where r_2 is the outer radius of the paper cup, r_3 is the combined outer radius of the cup and copper layer, k_{Cu} is the thermal conductivity of copper, and $T_{Cu}(t)$ is the temperature of the copper layer in contact with the SEBS polymer.

The temperature of the copper layer in contact with the SEBS polymer $T_{Cu}(t)$ was calculated according to Fourier's Law for cylindrical objects by using the following equation:

$$T_{Cu}(t) = \frac{q(t)\, ln\frac{r_4}{r_3}}{2\pi L k_{SEBS}} + T_{external}(t) \tag{15}$$

where r_4 is the combined outer radius of the cup, copper layer, and SEBS polymer, k_{SEBS} is the thermal conductivity of the SEBS polymer, and $T_{external}(t)$ is the temperature of the external surface of the SEBS polymer exposed to the surrounding environment.

The temperature of the external surface of the SEBS polymer exposed to the surrounding environment $T_{external}(t)$ was calculated according to Fourier's Law for cylindrical objects by using the following equation:

$$T_{external}(t) = \frac{q(t)}{2\pi r_4 L h_{eff}} + T_{environment} \tag{16}$$

where h_{eff} is the effective heat transfer coefficient.

The temperature of the coffee inside the composite-covered cup $T_{internal}(t)$ was updated by substituting equations *(13) – (16* into equation *(12)* and calculated by using the following equation:

$$T_{internal}(t) = \frac{q(t)}{2\pi L}\left(\frac{1}{h_{coffee} r_1} + \frac{ln\frac{r_2}{r_1}}{k_p} + \frac{ln\frac{r_3}{r_2}}{k_{Cu}} + \frac{ln\frac{r_4}{r_3}}{k_{SEBS}} + \frac{1}{h_{eff} r_4}\right) + T_{environment} \tag{17}$$

The overall heat transfer coefficient for the coffee in the composite-covered cup *U* was defined from equation *(17)* and calculated by using the following equation:

$$U = \frac{1}{h_{coffee} r_1} + \frac{ln\frac{r_2}{r_1}}{k_p} + \frac{ln\frac{r_3}{r_2}}{k_{Cu}} + \frac{ln\frac{r_4}{r_3}}{k_{SEBS}} + \frac{1}{h_{eff} r_4} \tag{18}$$

The temperature of the coffee inside the composite-covered cup $T_{internal}(t)$ was updated by substituting equation *(18)* into equation *(17)* and calculated by using the following equation:

$$T_{internal}(t) = \frac{q(t)}{2\pi L} U + T_{environment} \quad (19)$$

The energy balance for the system, i.e., the composite-covered, coffee-filled cup and the surrounding environment, was defined according to the following equation:

$$\frac{d}{dt}\left(T_{internal}(t)\right) = -\frac{1}{mc_w} q(t) \quad (20)$$

where m is the mass of the coffee and c_w is the heat capacity of coffee (water).

The energy balance for the system was updated by substituting equation *(19)* into equation *(20)* and calculated by using the following equation:

$$\frac{d}{dt}\left(T_{internal}(t)\right) = -\frac{1}{mc_w} \frac{(T_{internal}(t) - T_{environment})2\pi L}{U} \quad (21)$$

The temperature of the coffee inside the composite-covered cup $T_{internal}(t)$ was defined by solving equation *(21)* under the initial condition of $T_{internal}(t = 0) = 85°C = 358\,K$ and calculated by using the following equation:

$$T_{internal}(t) = (T_{internal}(t = 0) - T_{environment})e^{-\frac{1}{mc_w}\frac{2\pi L}{U}t} + T_{environment} \quad (22)$$

The cooling rate constant *k* was calculated by using the following equation:

$$k = \frac{d(\ln{(T_{internal}(t) - T_{environment})})}{dt} \quad (23)$$

The above equations were used to calculate 1) the theoretical external and internal temperatures in **Supplementary Figures 14a** and **15a** and 2) the theoretical external and internal cooling rates in **Supplementary Figures 14b** and **15b** for coffee-filled cups not covered by a material, covered with composites under strains of 0 %, 10 %, 20 %, or 30 %, covered with an unstrained SEBS polymer film under a strain of 0 %, or covered with a metallized Mylar sheet under a strain of 0 %.

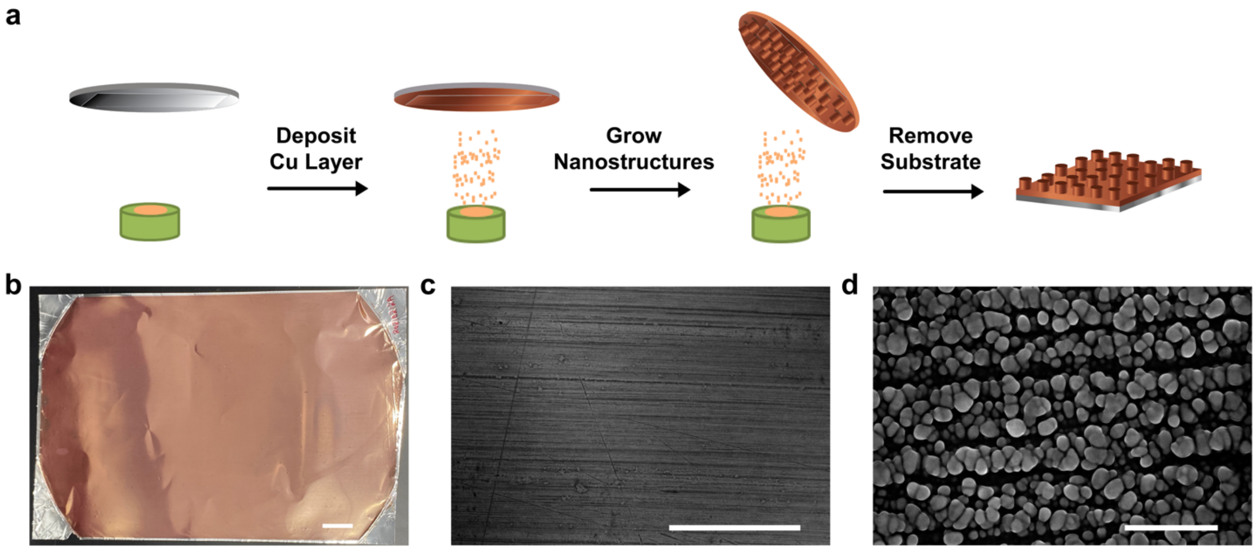

Supplementary Figure 1. a, A schematic illustrating the fabrication of substrate-bound nanostructured copper (Cu) films. The steps include the electron beam evaporation (deposition) of a planar copper layer onto an aluminum foil substrate, the growth of upright columnar copper nanostructures on top of the planar layer, and the removal of the substrate-bound nanostructured copper film from the deposition system. **b**, A representative digital camera picture of a substrate-bound nanostructured copper film. The scale bar is 2 cm. **c**, A representative top-down SEM image of a substrate-bound nanostructured copper film at low magnification. The scale bar is 500 µm. **d**, A representative top-down SEM image of a substrate-bound nanostructured copper film at high magnification. The scale bar is 500 nm.

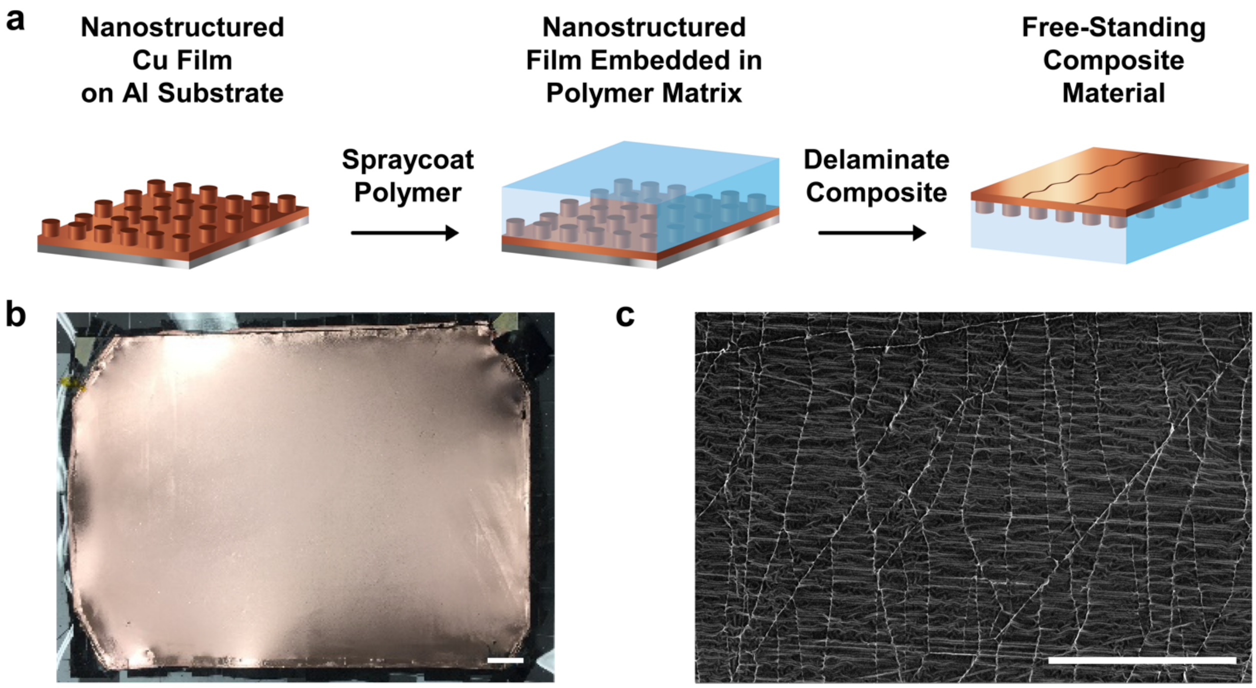

Supplementary Figure 2. a, A schematic illustrating the fabrication of the large-area composite materials. The steps include spraycoating of the SEBS matrix onto a substrate-bound nanostructured copper film and delamination of the resulting architecture from the support substrate. **b**, A representative digital camera picture of a large-area composite material mounted on a plastic frame. The scale bar is 2 cm. **c**, A representative top-down SEM image of the large-area composite material. The scale bar is 200 µm.

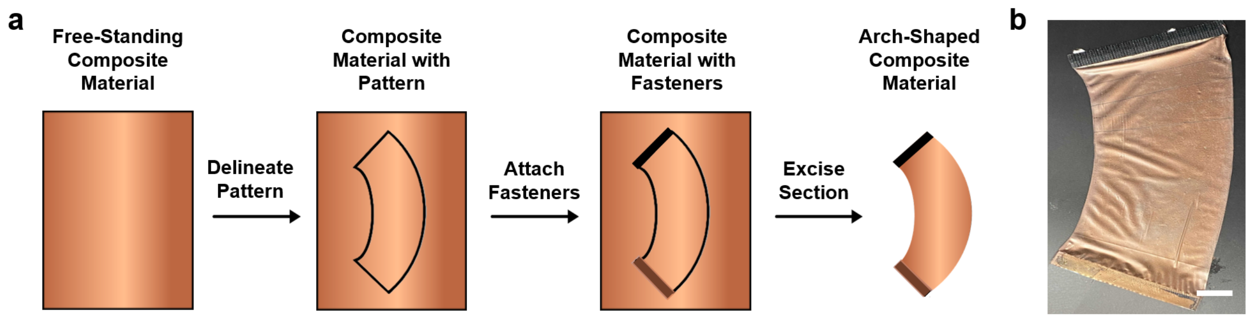

Supplementary Figure 3. a, A schematic illustrating the fabrication of a composite with an arch shape. The steps include delineating (drawing) a pattern on a composite material, attaching hook-and-loop components as fasteners to opposing sides of the composite material, and excising the fastener-modified section. **b**, A representative digital camera picture of an arch-shaped composite material. The scale bar is 2.5 cm.

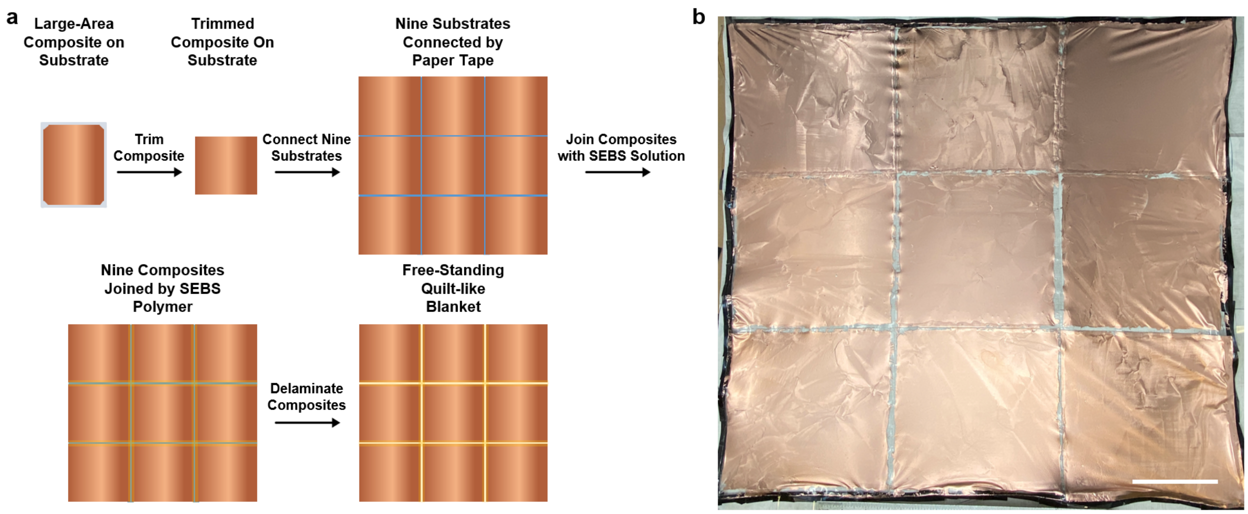

Supplementary Figure 4. **a**, A schematic illustrating the fabrication of composites in a blanket-like configuration. The steps include trimming of nine substrate-bound composites into smaller rectangles, connecting the nine trimmed composites' substrates together with adhesive tape while leaving small gaps, joining the nine composites by syringe-casting SEBS solutions into their intervening gaps, and simultaneously delaminating the nine composites from their support substrates as a single sheet. **b**, A representative digital camera picture of a blanket-like composite material. The scale bar is 10 cm.

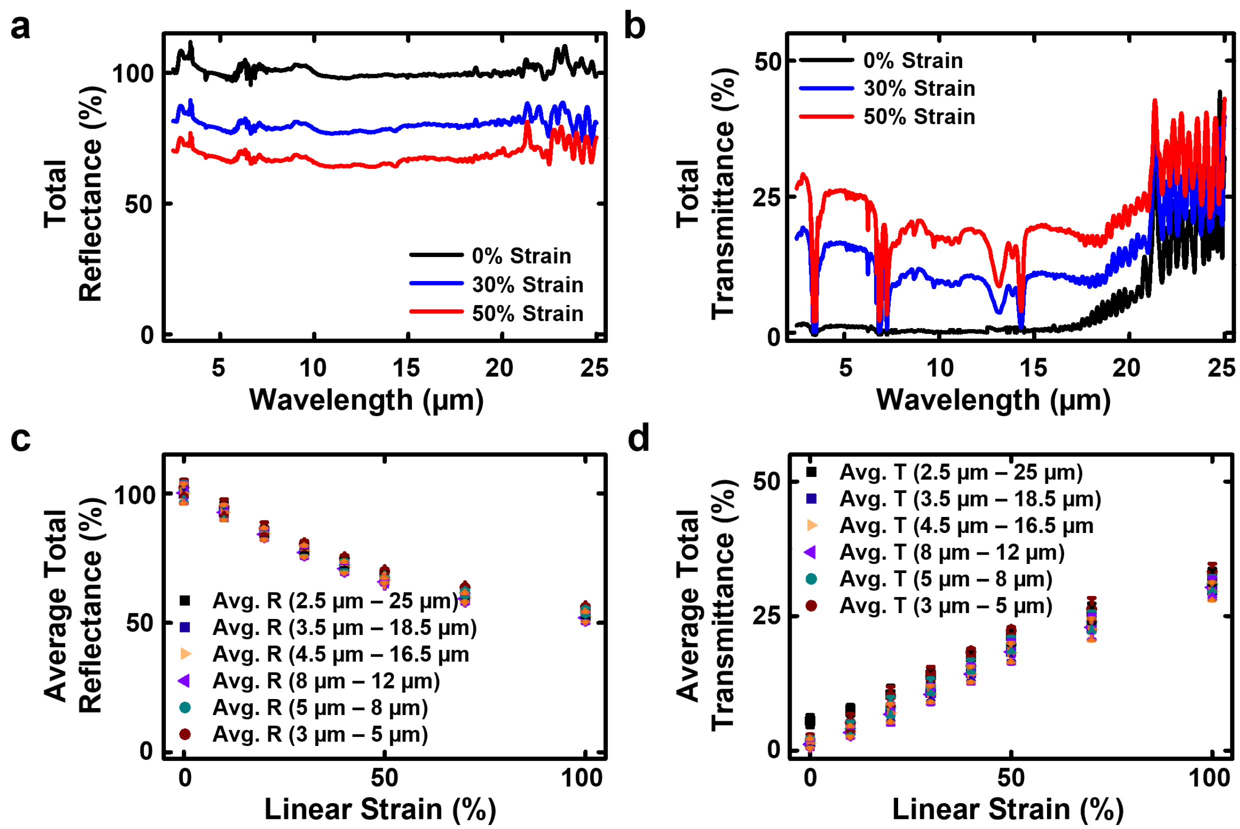

Supplementary Figure 5. a, The representative mid-infrared total reflectance spectra obtained for a composite material subjected to applied strains of 0 % (black), 30 % (blue), and 50 % (red). **b**, The representative mid-infrared total transmittance spectra obtained for a composite material subjected to applied strains of 0 % (black), 30 % (blue), and 50 % (red). **c**, The average values of the total reflectance R for the composite materials at different applied strains of ≤ 100 % over the wavelength ranges of 2.5 µm – 25 µm (black squares), 3.5 µm – 18.5 µm (dark blue squares), 4.5 µm – 16.5 µm (light orange triangles), 8 µm – 12 µm (purple triangles), 5 µm – 8 µm (turquoise circles), and 3 µm – 5 µm (brown circles). **d**, The average values of the total transmittance T for the composite materials at different applied strains of ≤ 100 % over the wavelength ranges of 2.5 µm – 25 µm (black squares), 3.5 µm – 18.5 µm (dark blue squares), 4.5 µm – 16.5 µm (light orange triangles), 8 µm – 12 µm (purple triangles), 5 µm – 8 µm (turquoise circles), and 3 µm – 5 µm (brown circles). The error bars in **c** and **d** represent standard deviations.

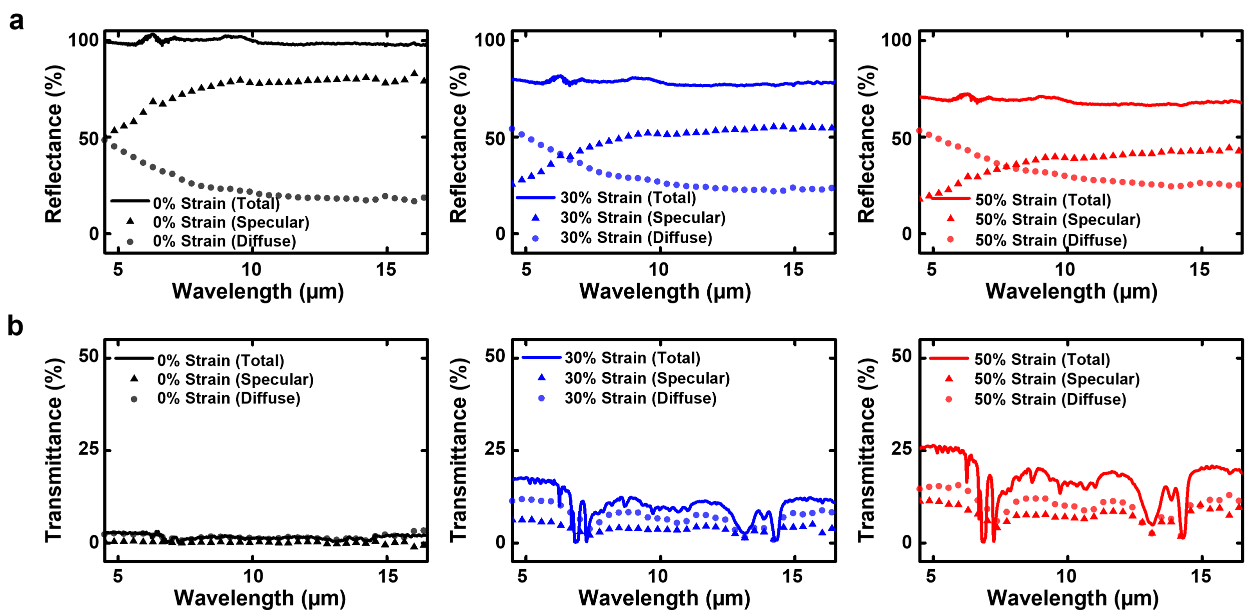

Supplementary Figure 6. a, Left: The representative total (black solid line), specular (black triangles), and diffuse (black circles) reflectance spectra obtained for a composite material subjected to an applied strain of 0 %. Middle: The representative total (blue solid line), specular (blue triangles), and diffuse (blue circles) reflectance spectra obtained for a composite material subjected to an applied strain of 30 %. Right: The representative total (red solid line), specular (red triangles), and diffuse (red circles) reflectance spectra obtained for a composite material subjected to an applied strain of 50 %. **b**, Left: The representative total (black solid line), specular (black triangles), and diffuse (black circles) transmittance spectra obtained for a composite material subjected to an applied strain of 0 %. Middle: The representative total (blue solid line), specular (blue triangles), and diffuse (blue circles) transmittance spectra obtained for a composite material subjected to an applied strain of 30 %. Right: The representative total (red solid line), specular (red triangles), and diffuse (red circles) transmittance spectra obtained for a composite material subjected to an applied strain of 50 %.

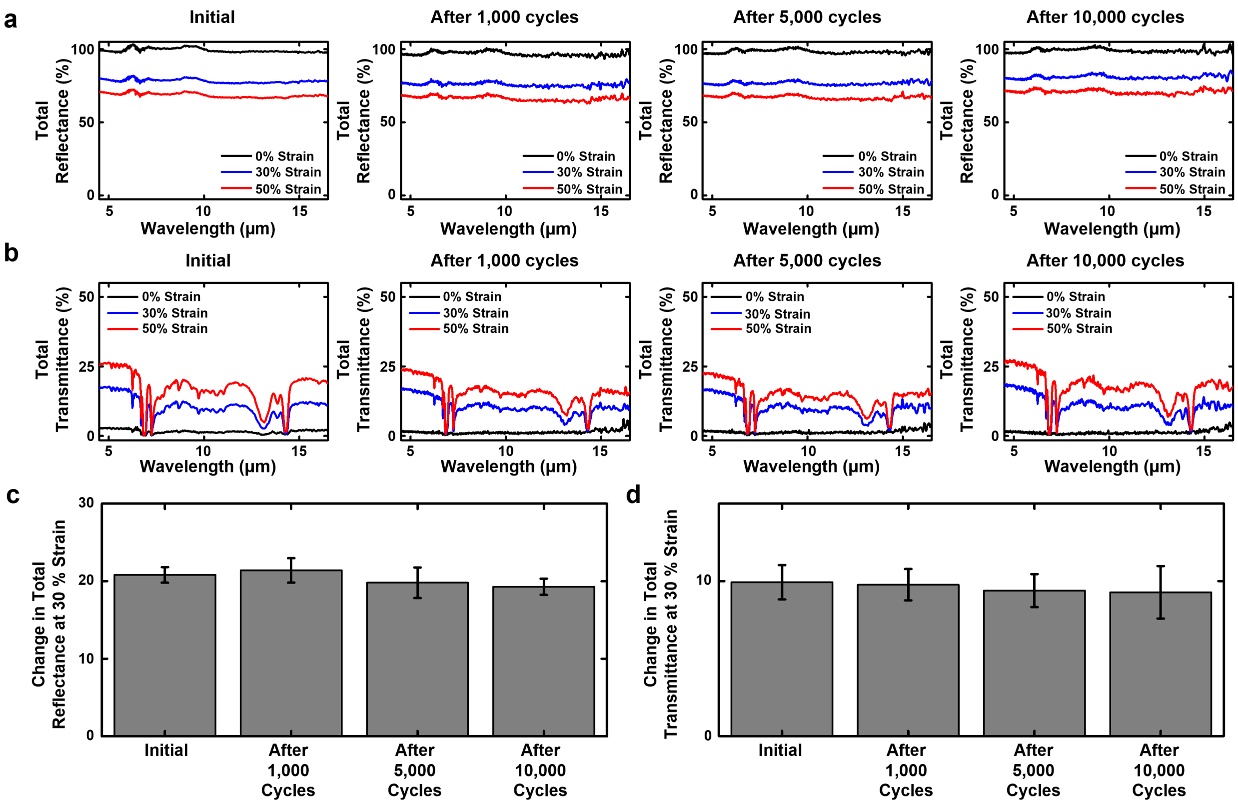

Supplementary Figure 7. **a**, The representative total reflectance spectra obtained for a composite material subjected to applied strains of 0 % (black), 30 % (blue), and 50 % (red) initially, after 1,000 actuation cycles, after 5,000 actuation cycles, and after 10,000 actuation cycles (from left to right). **b**, The representative total transmittance spectra obtained for a composite material under applied strains of 0 % (black), 30 % (blue), and 50 % (red) initially, after 1,000 actuation cycles, after 5,000 actuation cycles, and after 10,000 actuation cycles (from left to right). **c**, The average changes in the total reflectance at an applied strain of 30 % for composite materials initially, after 1,000 actuation cycles, after 5,000 actuation cycles, and after 10,000 actuation cycles. **d**, The average changes in the total transmittance at an applied strain of 30 % obtained for composite materials initially, after 1,000 actuation cycles, after 5,000 actuation cycles, and after 10,000 actuation cycles. The error bars in **c** and **d** represent standard deviations.

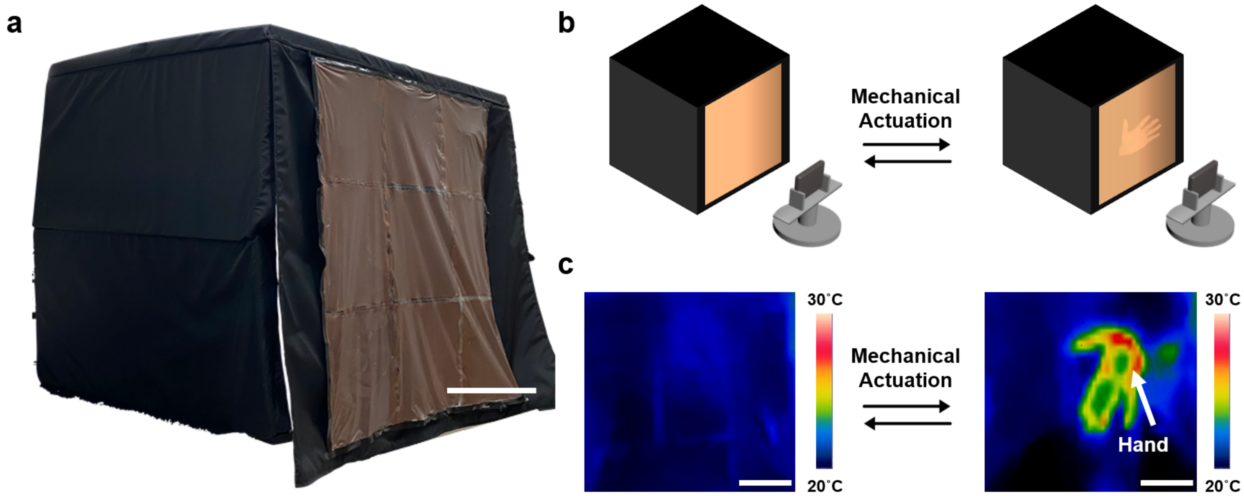

Supplementary Figure 8. a, A representative digital camera picture of a blanket-like composite integrated within a packaging-type enclosure. The scale bar is 15 cm. **b**, An illustration of an enclosure-integrated blanket-like composite, which is undergoing monitoring with a thermal infrared camera, before (left) and after (right) mechanical actuation, i.e., local deformation by a hand. **c**, Representative thermal infrared camera pictures obtained for an enclosure-integrated blanket-like composite before (left) and after (right) mechanical actuation, i.e., successful local deformation by a hand. The scale bars are 15 cm.

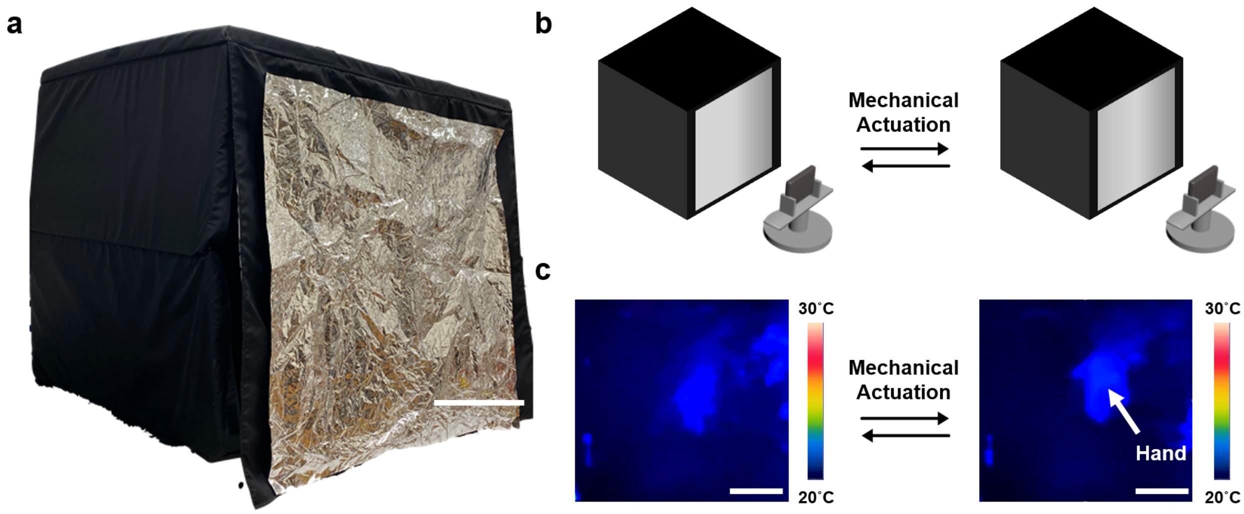

Supplementary Figure 9. a, A representative digital camera picture of a space blanket integrated within a packaging-type enclosure. The scale bar is 15 cm. **b**, An illustration of an enclosure-integrated space blanket, which is undergoing monitoring with a thermal infrared camera, before (left) and after (right) attempted mechanical actuation by a hand. **c**, Representative thermal infrared camera pictures obtained for an enclosure-integrated space blanket before (left) and after (right) mechanical actuation, i.e., attempted local deformation by a hand. The scale bars are 15 cm.

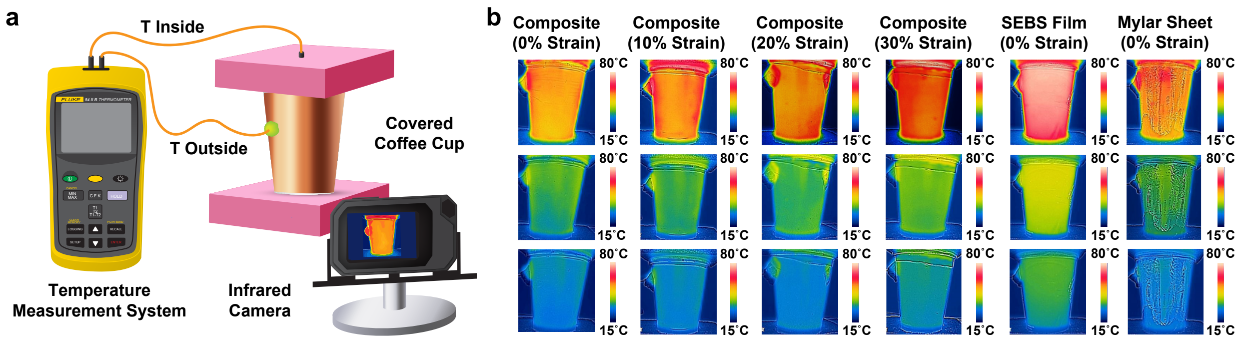

Supplementary Figure 10. a, An illustration of a cup covered with a composite material and filled with coffee, which is being monitored by a thermal infrared camera and a system that measures the external and internal temperatures. **b**, The representative time-lapse thermal infrared camera pictures obtained for covered coffee-filled cups after 0 min (top row), 60 min (middle row), and 90 min (bottom row). The cups are covered with composite materials under strains of 0 %, 10 %, 20 %, or 30 %, an SEBS polymer film under a strain of 0 %, and a metallized Mylar sheet under a strain of 0 % (from left to right). The cups featured thermocouples attached to their exteriors and positioned within their interiors.

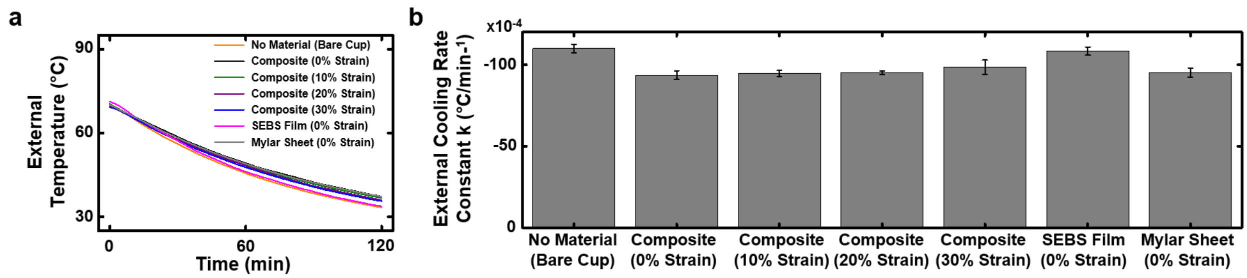

Supplementary Figure 11. a, The external temperatures measured as a function of time for coffee-filled cups not covered by a material (orange), covered by a composite material under a strain of 0 % (black), covered by a composite material under a strain of 10 % (green), covered by a composite material under a strain of 20 % (purple), covered by a composite material under a strain of 30 % (blue), covered by an SEBS polymer film under a strain of 0 % (pink), and covered by a metallized Mylar sheet under a strain of 0 % (grey). **b**, The average external cooling rates measured for coffee-filled cups not covered by a material, covered by composite materials under strains of 0 %, 10 %, 20 %, or 30 %, covered by an SEBS polymer film under a strain of 0 %, or covered by a metallized Mylar sheet under a strain of 0 % (from left to right). The error bars in **b** represent standard deviations.

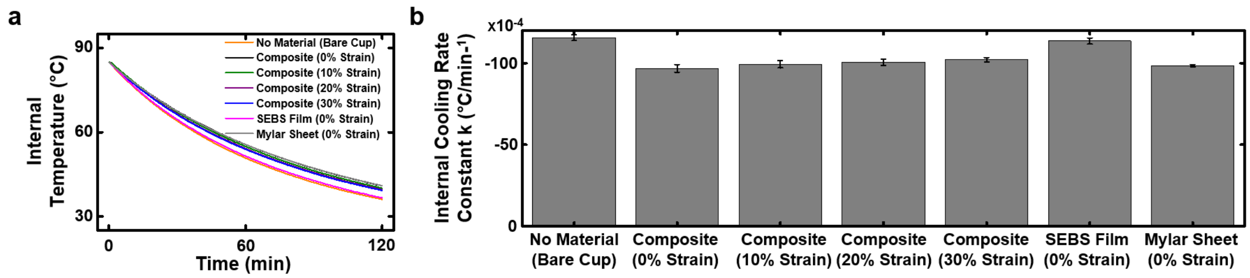

Supplementary Figure 12. a, The internal temperatures measured as a function of time for coffee-filled cups not covered by a material (orange), covered by a composite material under a strain of 0 % (black), covered by a composite material under a strain of 10 % (green), covered by a composite material under a strain of 20 % (purple), covered by a composite material under a strain of 30 % (blue), covered by an SEBS polymer film under a strain of 0 % (pink), and covered by a metallized Mylar sheet under a strain of 0 % (grey). **b**, The average internal cooling rates measured for coffee-filled cups not covered by a material, covered by composite materials under strains of 0 %, 10 %, 20 %, or 30 %, covered by an SEBS polymer film under a strain of 0 %, or covered by a metallized Mylar sheet under a strain of 0 % (from left to right). The error bars in **b** represent standard deviations.

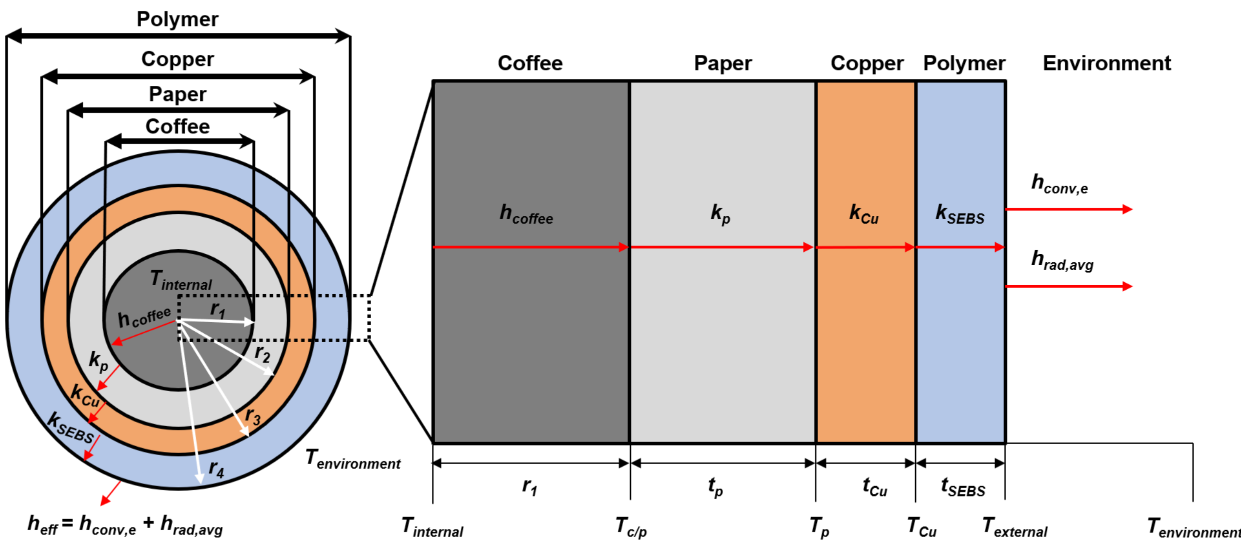

Supplementary Figure 13. An illustration of the configuration used to theoretically calculate heat transfer between the composite material-covered coffee-filled cups and the surrounding environment. The associated equations and parameters are explicitly listed or defined in **Supplementary Note 2**, **Supplementary Table 2**, and/or **Supplementary Table 3**. Note that analogous configurations were used for theoretical calculations involving SEBS polymer film-covered, unstrained metallized Mylar sheet-covered, and bare (uncovered) coffee-filled cups.

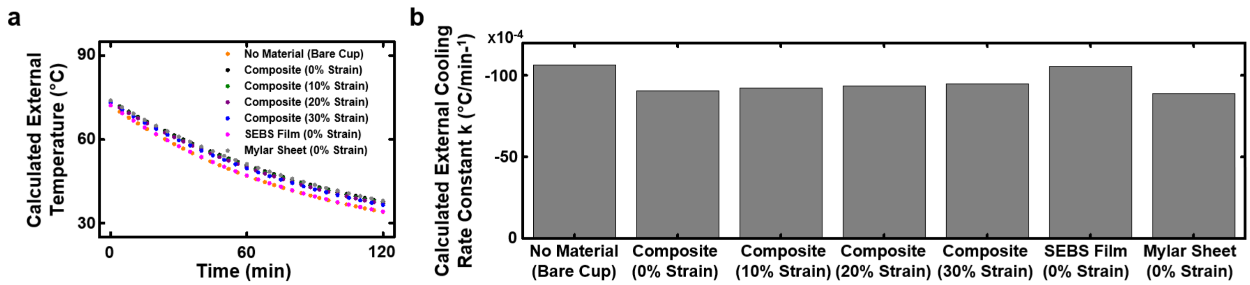

Supplementary Figure 14. a, The external temperatures theoretically calculated for coffee-filled cups not covered by a material (orange circles), covered by a composite material under a strain of 0 % (black circles), covered by a composite material under a strain of 10 % (green circles), covered by a composite material under a strain of 20 % (purple circles), covered by a composite material under a strain of 30 % (blue circles), covered by an SEBS polymer film under a strain of 0 % (pink circles), and covered by a metallized Mylar sheet under a strain of 0 % (grey circles). **b**, The external cooling rates theoretically calculated for coffee-filled cups not covered by a material, covered by composite materials under strains of 0 %, 10 %, 20 %, or 30 %, covered by an SEBS polymer film under a strain of 0 %, or covered by a metallized Mylar sheet under a strain of 0 % (from left to right). Note the agreement of the calculated values with the experimentally measured ones in **Supplementary Figure 11**.

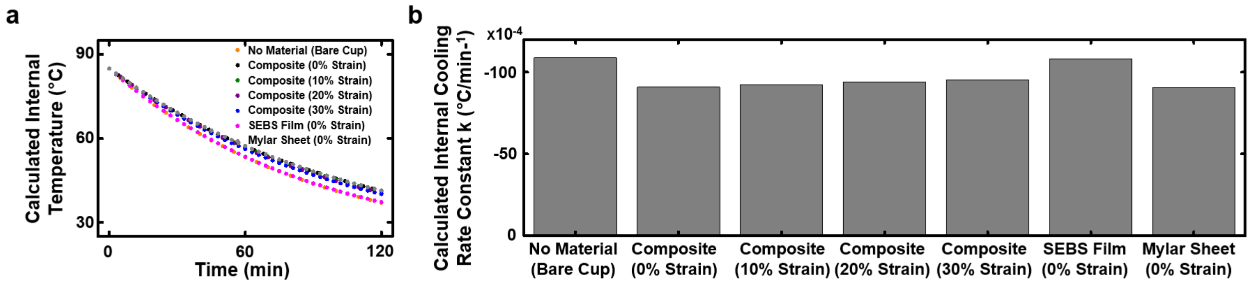

Supplementary Figure 15. a, The internal temperatures theoretically calculated for coffee-filled cups not covered by a material (orange circles), covered by a composite material under a strain of 0 % (black circles), covered by a composite material under a strain of 10 % (green circles), covered by a composite material under a strain of 20 % (purple circles), covered by a composite material under a strain of 30 % (blue circles), covered by an SEBS polymer film under a strain of 0 % (pink circles), and covered by a metallized Mylar sheet under a strain of 0 % (grey circles). **b**, The internal cooling rates theoretically calculated for coffee-filled cups not covered by any material, covered by composite materials under strains of 0 %, 10 %, 20 %, or 30 %, covered by an SEBS polymer film under a strain of 0 %, or covered by a metallized Mylar sheet under a strain of 0 % (from left to right). Note the agreement of the calculated values with the experimentally measured ones in **Supplementary Figure 12**.

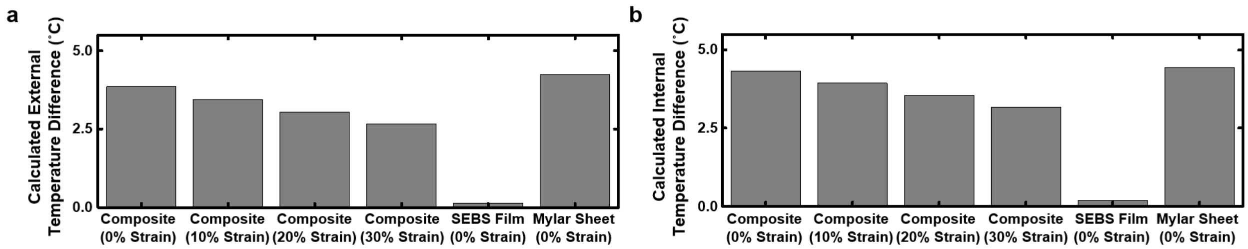

Supplementary Figure 16. a, The theoretically calculated external temperature differences between various material-covered coffee-filled cups and analogous bare cups after 90 minutes. The coffee-filled cups were modeled as covered with unstrained and strained composites, unstrained SEBS polymer films, and unstrained metallized Mylar sheets. **b**, The theoretically calculated internal temperature differences between various material-covered coffee-filled cups and analogous bare cups after 90 minutes. The coffee-filled cups were modeled as covered by unstrained and strained composites, unstrained SEBS polymer films, and unstrained metallized Mylar sheets. Note the general agreement of the theoretically calculated values with the experimentally measured values in **Figure 5c,d**.

Supplementary Table 1. A comparison of the costs estimated for the manufacturing of metallized polymer sheets and the described composite materials in **Supplementary Note 1**. Note that $C_{MT,Composite}$, i.e., the total starting material costs provided for the composites, are estimated from direct vendor quotes for laboratory-scale production and would be substantially lowered by economies of scale.

Metallized Sheet Cost Parameter	***Historical Percentage of the Total Cost***	***Historical Costs for Metallized Sheets (per m²)***	***Composite Material Cost Parameter***	***Estimated Cost for the Composite Materials (per m²)***
$C_{L,PS}$	3 % to 12 % %[S11]	~ $ 0.002 to ~ $ 0.018[S11]	$C_{L,Composite}$	~ $ 0.002 to ~ $ 0.018
$C_{MT,PS}$	60 % to 73 %[S11]	~ $ 0.04 to ~ $ 0.09[S11,S12]	$C_{MT,Composite}$	~ $ 0.1 to ~ $ 0.13
$C_{MF,PS}$	24 % to 28 %[S11]	~ $ 0.013 to ~ $ 0.042[S11]	$C_{MF,Composite}$	~ $ 0.013 to ~ $ 0.042
$\mathbf{C_{Total,PS}}$	**~ 100 %**	**~ $ 0.055 – ~ $ 0.15**	$\mathbf{C_{Total,Composite}}$	**~ $ 0.115 – ~ $ 0.19**

Supplementary Table 2. Compilation of the various measured, calculated, and estimated parameters used to theoretically calculate heat transfer between the material-covered coffee-filled cups and the surrounding environment in **Supplementary Note 2**.

Parameter Name	***Symbol***	***Value***	***Units***
$Convective\ heat\ transfer\ coefficient\ of\ coffee\ (water)$[S13]	h_{coffee}	290	$[\frac{W}{m^2K}]$
$Convective\ heat\ transfer\ coefficient\ of\ air$[S14]	$h_{conv,e}$	11	$[\frac{W}{m^2K}]$
$Average\ radiative\ heat\ transfer\ coefficient$	$h_{rad,avg}$	Composite (0% Strain) + Paper = 2.5 Composite (10% Strain) + Paper = 2.7 Composite (20% Strain) + Paper = 3.0 Composite (30% Strain) + Paper = 3.3 SEBS Polymer + Paper = 5.7 Metallized Mylar Sheet + Paper = 3.0 Paper = 5.8	$[\frac{W}{m^2K}]$
$Thermal\ conductivity\ of\ paper$[S15]	k_p	0.06	$\left[\frac{W}{mK}\right]$

Thermal conductivity of copper[S13]	k_{Cu}	385	$\left[\frac{W}{mK}\right]$
Thermal conductivity of the SEBS polymer[S16]	k_{SEBS}	0.19	$\left[\frac{W}{mK}\right]$
Thermal conductivity of the metallized Mylar sheet[S17]	k_{MS}	0.15	$\left[\frac{W}{mK}\right]$
Boltzmann constant	σ	5.67 × 10^{-8}	$[\frac{W}{m^2K^4}]$
Paper thickness	t_p	0.7	$[mm]$
Copper thickness	t_{Cu}	0.00011	$[mm]$
SEBS Polymer thickness	t_{SEBS}	0.02989	$[mm]$
Metallized Mylar sheet thickness	t_{MS}	0.0105	$[mm]$
Inner radius of the cup	r_1	34.95	$[mm]$
Height of the cup	L	87.47	$[mm]$
Volume of coffee	V_{coffee}	0.000335	$[m^3]$
Specific heat capacity of coffee (water)[S18]	c_w	4184	$[\frac{J}{kgK}]$
Initial temperature of the coffee	$T_{internal}$ $(t = 0)$	358	$[K]$
Temperature of the environment	$T_{environment}$	293	$[K]$

Supplementary Table 3. Compilation of the average reflectance, transmittance, and emittance values used to theoretically calculate heat transfer between material-covered coffee-filled cups and the surrounding environment in **Supplementary Note 2**. Note that the reflectance and transmittance values were obtained from experimental measurements performed for bare (uncovered) paper cups, SEBS polymer films affixed to paper cups, metallized Mylar sheets affixed to paper cups, and various composites affixed to paper cups.

Material Type	***Reflectance, ρ***	***Transmittance, τ***	***Emittance, ε***
Bare Paper Cup	0.14	0.01	0.85
SEBS Polymer Film on a Paper Cup	0.16	0.01	0.83
Metallized Mylar Sheet on a Paper Cup	0.55	0.01	0.44
Composite at 0 % Strain on a Paper Cup	0.63	0.01	0.36
Composite at 10 % Strain on a Paper Cup	0.59	0.01	0.40
Composite at 20 % Strain on a Paper Cup	0.55	0.01	0.44
Composite at 30 % Strain on a Paper Cup	0.51	0.01	0.48

Supplementary References.

S1. Robertson, G. L. *Food Packaging: Principles and Practice* 3rd edn (CRC Press, 2016); https://doi.org/10.1201/b21347

S2. Saba, N., Jawaid, M. & Thariq, M. *Biopolymers and Biocomposites from Agro-Waste for Packaging Applications* (Elsevier, 2021); https://doi.org/10.1016/C2019-0-00969-7

S3. Bishop, C. A. & Mount, E. M. in *Multilayer Flexible Packaging* (ed Wagner, J. R.) 185–202 (Elsevier, 2010); https://doi.org/10.1016/B978-0-8155-2021-4.10014-0

S4. Bayus, J., Ge, C. & Thorn, B. A preliminary environmental assessment of foil and metallized film centered laminates. *Resour. Conserv. Recycl.* **115**, 31–41 (2016).

S5. Vasile, C. Polymeric nanocomposites and nanocoatings for food packaging: a review. *Materials (Basel).* **11**, 1834 (2018).

S6. Mbam, S. O., Nwonu, S. E., Orelaja, O. A., Nwigwe, U. S. & Gou, X.-F. Thin-film coating; historical evolution, conventional deposition technologies, stress-state micro/nano-level measurement/models and prospects projection: a critical review. *Mater. Res. Express* **6**, 122001 (2019).

S7. Anukiruthika, T. *et al.* Multilayer packaging: advances in preparation techniques and emerging food applications. *Compr. Rev. Food Sci. Food Saf.* **19**, 1156–1186 (2020).

S8. Bader, M. G. Selection of composite materials and manufacturing routes for cost-effective performance. *Compos. Part A Appl. Sci. Manuf.* **33**, 913–934 (2002).

S9. Esawi, A. M. K. & Ashby, M. F. Cost estimates to guide pre-selection of processes. *Mater. Des.* **24**, 605–616 (2003).

S10. Centea, T. & Nutt, S. R. Manufacturing cost relationships for vacuum bag-only prepreg processing. *J. Compos. Mater.* **50**, 2305–2321 (2016).

S11. IHS Markit. *Specialty Plastic Films – Process Economics Program Report 159B (economic values updated in 2021)* (1993); https://ihsmarkit.com/products/chemical-technology-pep-specialty-plastic-films-1993.html.

S12. Decker, W., Roy, D., Voght, C., Roy, C. & Dabbert, P. Metallized polymer films as replacement for Aluminum foil in packaging applications. *Proc. Annu. Tech. Conf. Vac. Coaters* **47**, 594–599 (2004).

S13. Powell, R. W., Ho, C. Y. & Liley, P. E. *Thermal Conductivity of Selected Materials*. (Washington, DC: US Department of Commerce, National Bureau of Standards, 1966).

S14. Kosky, P., Balmer, R. T., Keat, W. D., & Wise, G. *Exploring Engineering: An Introduction to Engineering and Design* 3rd edn (*Academic Press*, 2013); https://doi.org/10.1016/C2011-0-04445-9

S15. Lavrykov, S. A. & Ramarao, B. V. Thermal properties of copy paper sheets. *Dry. Technol.* **30**, 297–311 (2012).

S16. Tsutsumi, N. in *Structure and Properties of Multiphase Polymeric Materials* (eds Araki, T., Shibayama, M. & Tran-Cong, Q.) 393-422 (Marcel-Dekker, Inc., 1998).

S17. Meseguer, J., Pérez-Grande, I. & Sanz-Andrés, A. *Spacecraft Thermal Control* (Woodhead Publishing, 2012).

S18. Taylor, S. A. & Jackson, R. D. in *Methods Soil Anal. Part 1 Phys. Mineral. Methods* (ed Klute, A.) 941–944 (2018); https://doi.org/10.2136/sssabookser5.1.2ed.c38